Available online at www.sciencedirect.com
SCIENCE DIRECT
Polymer 46 (2005) 10544–10552
polymer
www.elsevier.com/locate/polymer

Copoly(aryl ether)s with electron-transporting 2,7-bis(3-(trifluoromethyl) phenyl)-9,9-dihexylfluorene segments: Synthesis, optical, and electrochemical properties

Shinn-Horng Chen, Yun Chen*

Department of Chemical Engineering, National Cheng Kung University, No. 1, Da-Syue Road, 701 Tainan, Taiwan, ROC

Received 12 May 2005; received in revised form 31 July 2005; accepted 6 August 2005
Available online 19 August 2005

Abstract

We prepared and characterized three new copoly(aryl ether)s (**P1**–**P3**) consisting of alternate electron-transporting 2,7-bis(3-(trifluoromethyl)phenyl)-9,9-dihexylfluorene and hole-transporting fluorophores (**P1**: 3,6-distyryl-*N*-2-ethylhexylcarbazole; **P2**: 2,7-distyryl-9,9-dihexylfluorene; **P3**: 1,4-distyryl-2,5-dihexylbenzene) separated by ether spacers. The copolymers were soluble in common organic solvents such as chloroform, NMP, and 1,1,2,2-tetrachloroethane and exhibited good thermal stability with T_ds higher than 360 °C. Optical properties of **P1**–**P3** were investigated by comparing their absorption and photoluminescence spectra with those of compositional model compounds **M1**–**M4**. The emissions of **P1**–**P3** are originated from both fluorophores (**P1**) or dominated by fluorophores with longer emissive wavelength via efficient energy transfer (**P2** and **P3**). Cyclic voltammetric investigations confirm that incorporation of isolated hole- and electron-transporting segments leads to simultaneous enhancement of electron and hole affinity in these copoly(aryl ether)s. The HOMO and LUMO energy levels of **P1**–**P3** are −5.15, −5.28, −5.17 and −3.04, −3.06, −3.08 eV, respectively, and double-layer light emitting diodes of **P1**–**P3** reveal emission maxima around 450–500 nm.

Keywords: Electrochemistry; Light-emitting diodes (LED); Polyethers

1. Introduction

Conjugated polymers contain delocalized π-electrons bonding along backbone that support the mobility of charges and possess semiconducting properties. Electroluminescence (EL) from conjugated polymers has been subject of recent extensive studies [1–7]. The development of high-performance materials is also a key issue for fabrication of efficient EL devices. Among EL materials, isolated or π-conjugated polymers with donor-acceptor architectures are currently of interest because the electron and hole affinity can be enhanced simultaneously or controlled independently [8,9].

However, fully conjugated polymers are actually consisting of chromophores with different energy gaps because the effective conjugation length is statistically distributed. Thus the chromophores with lower energy gaps will be the emitting species via reabsorption or energy transfer [10,11]. Confinement of conjugation into a well-defined length of polymeric chain is one of the most successful strategies to solve this problem [12–15]. Furthermore, one common tactic to balance charge mobility or reduce operation voltage of efficient EL devices is to fabricate multi-layer EL devices, which insert hole- and/or electron-transporting layers between the emissive layer and electrodes [16–18]. However, the fabrication of multi-layer devices is often limited by fewer suitable solvents, which will not dissolve previously cast polymeric film. The other tactic is to improve the device efficiency by incorporation of electron- or hole-transporting segments into the side-chain or backbone of the conjugated polymers.

In our previous work, we reported copoly(aryl ether)s consisting of alternate isolated electron-transporting/emissive segments and hole-transporting/emissive segments. Both the electron and hole affinity of these copolymers could be enhanced, and the barriers of charge injection from

* Corresponding author. Tel./fax: +886 6 208 5843.
E-mail address: yunchen@mail.ncku.edu.tw (Y. Chen).

0032-3861/$ - see front matter © 2005 Elsevier Ltd. All rights reserved.
doi:10.1016/j.polymer.2005.08.018

the aluminum cathode and ITO anode could be decreased successfully. The ether spacers confine the conjugation range effectively and give rise to polymers emitting blue light [19–22].

Poly(*p*-phenylenevinylene) (PPV) and their derivatives have been widely recognized as one of the most potential candidate materials for EL application due to their unique processability and high luminescence [23–32]. Recently, polyfluorenes (PFs) have been introduced as a prospective emitting layer with emission wavelengths primarily in the blue spectral region. PFs are more thermally stable than PPV and display high PL efficiencies both in solution and in solid films [33–38]. Moreover, carbazole derivatives are well-known hole-transporting materials, which can be utilized in EL devices to promote charge mobility [39–41].

In this work, we synthesized and well characterized three novel poly(aryl ether)s **P1**–**P3**, which consisting of alternate hole-transporting segments [3,6-distyrylcarbazole, 2,7-distyrylfluorene, or 1,4-distyrylbenzene] and novel electron-transporting 2,7-bis(3-(trifluoromethyl)phenyl)-9,9-dihexylfluorene segments by nucleophilic aromatic substitution. Optical and electrochemical properties of these copoly(aryl ether)s are presented in detail. Moreover, we also compared optical properties of **P2** with analogous copolymer **P4**, which contain electron-transporting 3,3‴-bistrifluoromethylquaterphenyl groups, to discuss the improvement of interchain interaction in **P2**.

2. Experimental

2.1. Materials and measurements

The synthetic procedures of compounds **5**–**7**, model compounds **M2**–**M4**, and **P4** (Schemes 1 and 2) are described in the literatures elsewhere [25,35]. 9,9-

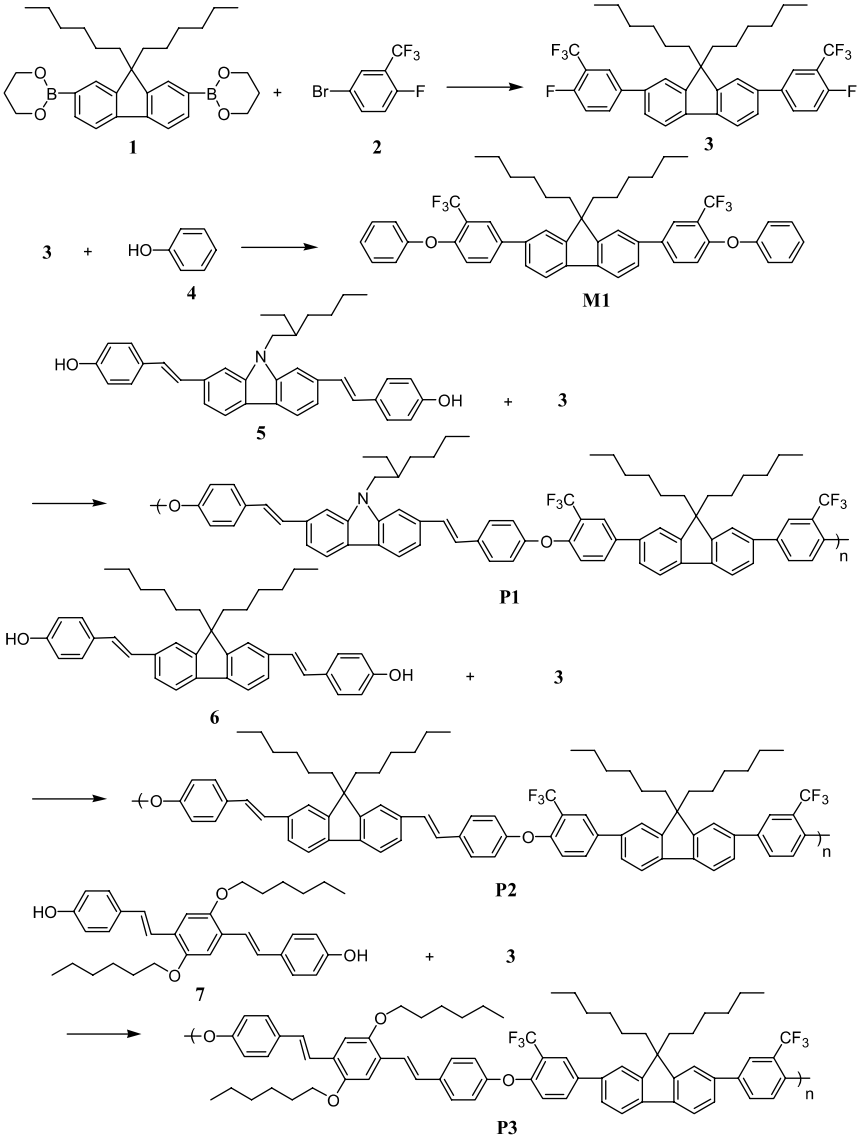

Scheme 1.

Dihexylfluorenr-2,7-bis(trimethyleneborate) (**1**, Aldrich Co.), 5-bromo-2-fluorobenzotrifluoride (**2**, Lancaster Co.), phenol (**4**, Lancaster Co.), *N*-methyl-2-pyrrolidone (NMP, Riedel-Dehaen Co.), *N*-cyclohexylpyrrolidone (CHP, Janssen Chimica Co.), chloroform ($CHCl_3$, Tedia Co.), tetrahydrofuran (THF, Tedia Co), and other solvents were used without any further purification.

All new compounds were identified by ^{1}H NMR, FT-IR, and elemental analysis (EA). The ^{1}H NMR spectra were recorded on a Bruker AMX-400 MHz FT-NMR, and chemical shifts are reported in ppm using tetramethylsilane (TMS) as an internal standard. The FT-IR spectra were measured as KBr disk on a Fourier transform infrared spectrometer, model Valor Ⅲ from Jasco. The elemental analysis was carried out on a Heraus CHN-Rapid elemental analyzer. The thermogravimetric analysis (TGA) of the polymers was performed under nitrogen atmosphere at a heating rate of 20 °C/min using a Perkin–Elmer TGA-7 thermal analyzer. Thermal properties of the polymers were carried out using a differential scanning calorimeter (DSC), Perkin–Elmer DSC 7, under nitrogen atmosphere at a heating rate of 20 °C/min. UV/visible spectra were measured with a Jasco V-550 spectrophotometer. The steady-state photoluminescence (PL) spectra were recorded on Hitachi F-4500 fluorescence spectrophotometer. The diagrammatic curves of cyclic voltammetry were recorded using a voltammetric analyzer, model CV-50W from BAS, under nitrogen atmosphere using ITO glass as working electrode, Ag/AgCl electrode as reference electrode and platinum wire electrode as auxiliary electrode supporting in 0.1 M $(n\text{-Bu})_4NClO_4$ in acetonitrile. The energy levels were calculated using the ferrocence (FOC) value of −4.8 eV with respect to vacuum level, which is defined as zero [42]. Two double-layer EL devices (ITO/PEDOT/**P1**–**P3**/Al) were also fabricated and their electroluminescent spectra were measured by Hitachi F-4500 fluorescence spectrophotometer.

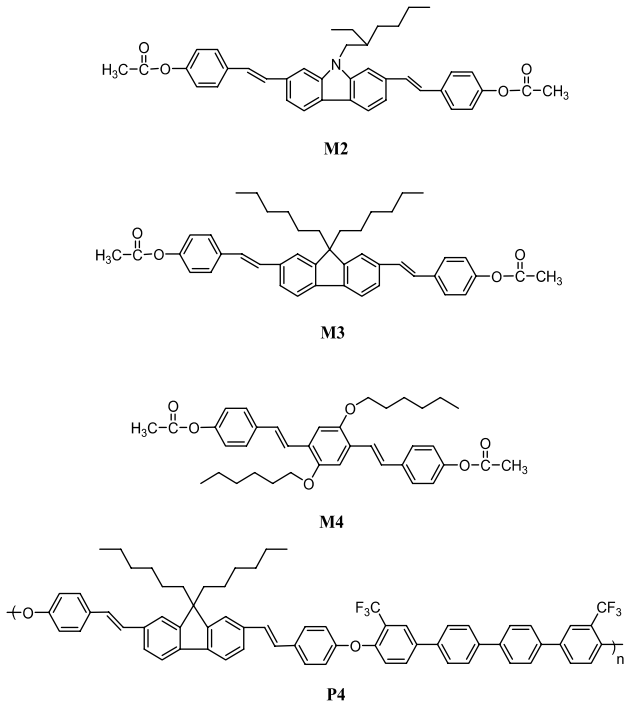

Scheme 2.

2.2. Monomer and model compounds synthesis (Scheme 1)

2.2.1. 2,7-Bis(4-fluoro-3-(trifluoromethyl)phenyl)-9,9-dihexyl-fluorene (*3*)

Compound **3** was synthesized by Suzuki biaryl coupling reaction as follows. To a two-necked 10-mL glass reactor was charged with 9,9-dihexylfluorene-2,7-bis(trimethyleneborate) (**1**: 0.50 g, 1 mmol), 5-bromo-2-fluorobenzotrifluoride (**2**: 0.51 g, 2.1 mmol), $Pd(PPh_3)_4$ (0.12 g, 0.1 mmol), 5 mL toluene, 2 mL ethanol (99%), and 1 mL 2 M Na_2CO_3(aq) under nitrogen atmosphere. The mixture was allowed to react at 80 °C for 13 h. After reaction was completely promoted it was poured into distilled water and extracted with chloroform. The organic layer was dried with anhydrous magnesium sulfate and vacuum concentrated. The crude product was purified by column chromatography and recrystallized from dichloromethane and ethyl acetate, and then dried in vacuum to afford compound **3** (65%). Mp: 111–112 °C. ^{1}H NMR (*d*-acetone, ppm): δ 8.11–8.04 (m, 4H, Ar H), 7.9–7.91 (m, 4H, Ar H), 7.78–7.69 (m, 2H, Ar H), 7.55–7.49 (m, 2H, Ar H), 2.23–2.18 (m, 4H, –CH_2–), 1.03 (s, 12H, –CH_2–), 0.75–7.74 (m, 4H, –CH_2–), 0.73–0.69 (m, H, –CH_3). FT-IR (film, cm^{-1}): 2959, 2927, 2857, 1622, 1513, 1335, 1249, 1129 (C–F), 1054, 810. Anal. Calcd (%) for $C_{39}H_{38}F_8$: C, 71.11; H, 5.81. Found: C, 71.40; H, 5.93.

2.2.2. 2,7-Bis(3-(trifluoromethyl)-4-phenoxyphenyl)-9,9-dihexyl-fluorene (*M1*)

To a two-necked 25-mL glass reactor was charged with **3** (0.329 g, 0.5 mmol), phenol (**4**: 0.19 g, 2 mmol), 6 mL DMF and K_2CO_3 (0.27 g, 2 mmol). The reaction mixture was then heated to 160 °C slowly and then reacted for 12 h. After the reaction was completely promoted, the reaction mixture was poured into a large amount of distilled water. The mixture was extracted with chloroform, and the extract was washed with distilled water, dried with anhydrous magnesium sulfate, and then concentrated under reduced pressure. The crude products were purified by column chromatography using ethyl acetate/*n*-hexane mixture as eluent. Evaporation of the eluent affords white solid of **M1** (52%). Mp: 131–132 °C. ^{1}H NMR (*d*-acetone, ppm): δ 8.08 (s, 2H, Ar H), 7.98–7.88 (m, 6H, Ar H), 7.77–7.70 (m, 2H, Ar H), 7.47–7.42 (m, 4H, Ar H), 7.24–7.19 (m, 2H, Ar H), 7.13–7.09 (m, 6H, Ar H), 2.23–2.17 (m, 4H –CH_2–), 1.03 (s, 12H, –CH_2–), 0.73–0.72 (m, 4H, –CH_2–), 0.70–0.68 (m, 6, –CH_3). FT-IR (film, cm^{-1}): 2955, 2932, 2857, 1587, 1490, 1335, 1253, 1129 (C–F), 1047, 814. Anal. Calcd (%) for $C_{51}H_{48}F_6O_2$: C, 76.83; H, 5.95. Found: C, 76.57; H, 6.30.

2.3. Polymerization (Scheme 2)

The copoly(aryl ether)s **P1–P3** were prepared from corresponding bis(fluoride) monomers **3** and bis(phenol)s (**5**, **6** or **7**) via nucleophilic substitution reaction using K_2CO_3 as catalyst. For example, to a two-necked 10-mL glass reactor was charged with **3** (0.50 mmol), bis(phenol) (0.50 mmol), 6 mL toluene, 3 mL solvent mixture of *N*-methyl-2-pyrrolidone (NMP)/*N*-cyclohexylpyrrolidone (CHP) (v/v = 1/1) and an excess amount of K_2CO_3 (0.166 g, 1.20 mmol). The polymerization temperatures and periods for **P1–P3** are listed in Table 1 and the trace water was removed by condensing in the Dean-Stark trap. Finally, the reaction mixture was dropped into 150 mL of methanol/distilled water (v/v = 2/1). The appearing precipitates were collected by filtration and further purified by extracting with isopropyl alcohol for 24 h using a Soxhlet extractor.

P1: ^{1}H NMR ($CDCl_3$, ppm): δ 8.26 (s, 2H, Ar H), 8.01 (s, 4H, Ar H), 7.76–7.53 (m, 12H, Ar H), 7.38–7.36 (m, 4H, Ar H), 7.18–7.03 (m, 8H, Ar H), 4.16 (s, 2H, –C*H*$_2$–), 2.03–2.01 (m, 4H, –C*H*$_2$–), 1.71 (m, 10H, –C*H*$_2$–), 1.36–1.35 (m, 7H, –C*H*$_2$–), 1.07 (s, 8H, –C*H*$_2$–), 0.89–0.73 (m, 12H, –C*H*$_3$). FT-IR (KBr pellet, cm^{-1}): 2929, 2820, 1626, 1515, 1332, 1249, 1135 (C–F), 1057, 819. Anal. Calcd (%) for $C_{73}H_{73}F_6NO_2$: C, 79.41; H, 6.49; N, 1.23. Found: C, 76.41; H, 6.39; N, 1.68.

P2: ^{1}H NMR ($CDCl_3$, ppm): δ 7.96 (m, 2H, Ar H), 7.81–7.66 (m, 6H, Ar H), 7.59–7.37 (m, 12H, Ar H), 7.17–6.87 (m, 10H, Ar H), 2.04 (s, 8H, –C*H*$_2$–), 1.09–1.07 (m, 24H, –C*H*$_2$–), 0.87 (s, 8H, –C*H*$_2$–), 0.76–0.74 (m, 12H, –C*H*$_3$). FT-IR (thin film, cm^{-1}): 2964, 2932, 2863, 1621, 1508, 1434, 1329, 1261, 1129 (C–F), 1051, 960. Anal. Calcd (%) for $C_{80}H_{82}F_6O_2$: C, 80.78; H, 6.95. Found: C, 77.38; H, 6.66.

P3: ^{1}H NMR ($CDCl_3$, ppm): δ 7.76–7.75 (m, 2H, Ar H), 7.60–7.52 (m, 6H, Ar H), 7.52–7.51 (m, 6H, Ar H), 7.37–7.35 (m, 2H, Ar H), 7.16–6.75 (m, 10H, Ar H), 4.07–4.05 (m, 4H, Ar H), 2.09–2.03 (m, 4H, –C*H*$_2$–), 1.70 (m, 12H, –C*H*$_2$–), 1.37–1.25 (m, 12H, –C*H*$_2$–), 1.06 (s, 8H, –C*H*$_2$–), 0.92–0.91 (m, 6H, –C*H*$_3$), 0.74–0.72 (m, 6H, –C*H*$_3$). FT-IR (KBr pellet, cm^{-1}): 2924, 2865, 1957, 1501, 1464, 1332, 1254 (C–O–C), 1131 (C–F), 1052, 966. Anal. Calcd (%) for $C_{73}H_{78}F_6O_4$: C, 77.36; H, 6.94. Found: C, 74.54; H, 6.84.

3. Results and discussion

3.1. Synthesis and characterization

Scheme 1 outlines the synthetic routes used to prepare the copoly(aryl ether)s (**P1–P3**), which are obtained from nucleophilic displacement reaction. The molecular weights of the resulting copoly(aryl ether)s are commonly higher than these obtained by Wittig reaction [43,44]. The weight-average molecular weights (M_w) of **P1–P3**, determined by gel permeation chromatography against polystyrene as standard, were 1.93×10^4, 10.3×10^4, and 8.47×10^4, respectively, with polydispersity index in the range of 2.53–3.13. **P1–P3** are readily soluble in common organic solvents such as chloroform, NMP and 1,1,2,2-tetrachloroethane. The polymerization results and characterization of **P1–P3** are summarized in Table 1. Thermal characteristic of **P1–P3** were evaluated by thermogravimetric analysis (TGA) and differential scanning calorimeter (DSC). TGA reveals that the decomposition temperatures T_ds (at 5% weight loss) are above 360 °C under nitrogen atmosphere. No melting temperature and obvious T_g (the glass transition temperature) can be observed below 300 °C on their DSC thermograms, suggesting **P1–P3** are basically amorphous polymeric materials.

3.2. Optical properties

The optical properties of copolymers **P1–P3** and model compounds **M1–M4** are summarized in Table 2. Fig. 1 shows the normalized absorption and photoluminescence spectra of model compounds **M1–M4**, which simulate the isolated fluorophores of **P1–P3**, correspondingly. For example, the backbone of **P1** is consisting of alternate 3,6-distyrylcarbazole (hole-transporting segments) and 2,7-bis(3-(trifluoromethyl)phenyl)-9,9-dihexylfluorene groups (electron-transporting segments), which can be properly simulated by **M2** and **M1**, respectively, in optical study. As summarized in Table 2, the absorption maxima of **M1–M4** in $CHCl_3$ locate at 335, 283, 380, 397 nm, and the main emission peaks appear at 372, 406, 433, 449 nm, respectively.

For isolated copolymers **P1–P3**, it is reasonable that their absorption and emission are originated from respective isolated fluorophores, i.e. electron-transporting and hole-

Table 1
Polymerization results and characterization of **P1–P3**

No.	Reaction temp. (°C)	Reaction time (h)	Yield (%)	M_n[a] ($\times10^4$)	M_w[a] ($\times10^4$)	PDI[a]	T_d[b] (°C)
P1	170	48	62	0.76	1.93	2.53	360
P2	170	48	75	3.29	10.3	3.13	445
P3	170	72	80	3.12	8.47	2.71	440

[a] M_n, M_w, and PDI of the polymers were determined by gel permeation chromatography using polystyrene standards in $CHCl_3$.
[b] The temperatures at 5% weight loss.

Table 2
Optical properties of model compounds and polymers

No.	UV–vis λ_{max}[a] solution (nm)	UV–vis λ_{max} film (nm)	PL λ_{max}[a] solution (nm)	PL λ_{max} film (nm)	Φ_{PL}[b]
P1	245, 336	335	372_s, 393, 411_s	414, 439	0.33
P2	378, 336_s	332, 378	420, 442, 472_s	423, 449, 479_s	0.93
P3	336, 388	396, 332	451, 478_s	459, 484	0.89
M1	335	–	372, 388, 416_s	–	
M2	283	–	406, 426_s	–	
M3	380	–	413, 433, 465_s	–	
M4	333, 397	–	449, 466_s	–	

[a] Concentration: 10^{-5} M in $CHCl_3$. Superscript s means the wavelength of the shoulder.
[b] These values were measured by the right-angle geometry using quinine sulfate (dissolved in 1 N H_2SO_4(aq) with a concentration of 10^{-5} M, assuming Φ_{PL} of 0.55) as a standard at 24–25 °C.

transporting segments. As observed in Fig. 2, in $CHCl_3$ each of **P1**–**P3** show absorption and photoluminescence (PL) peaks at 336, 378, 336, and 393, 442, 451 nm, respectively. Obviously, the emission spectrum of **P1** is contributed from both hole- and electron-transporting fluorophores. However, the PL spectra of **P2** and **P3**, exhibit only the emission bands contributed from hole-transporting fluorophores around 420–450 nm. For example, whether excited by 378 nm (Fig. 2) or by 335 nm [Fig. 3(a)], **P2** (in $CHCl_3$) shows only the emissions at 420 and 442 nm, which are attributed exclusively to hole-transporting 2,7-distyrylfluorene segments. Similar phenomenon can be found in **P3** [Figs. 2 and 3(b)]. This indicates that the emissions in **P2** and **P3** are dominated mainly by fluorophores with longer emissive wavelength. Appropriate explanation is that the excitation energy is transferred completely from electron-transporting

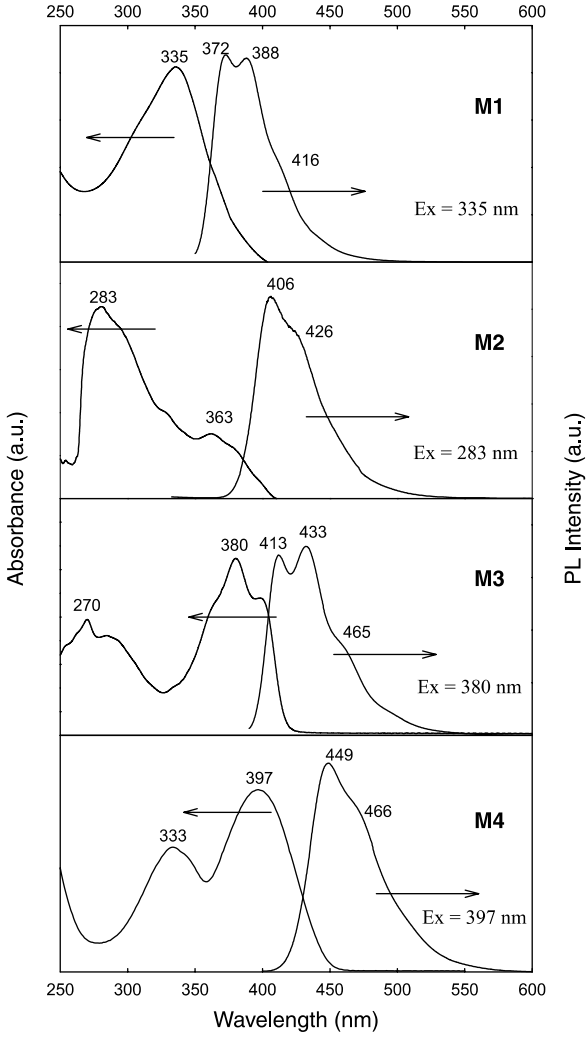

Fig. 1. Photoluminescence and UV–vis absorption spectra of model compounds **M1**–**M4** in $CHCl_3$ solutions of 1×10^{-5} M.

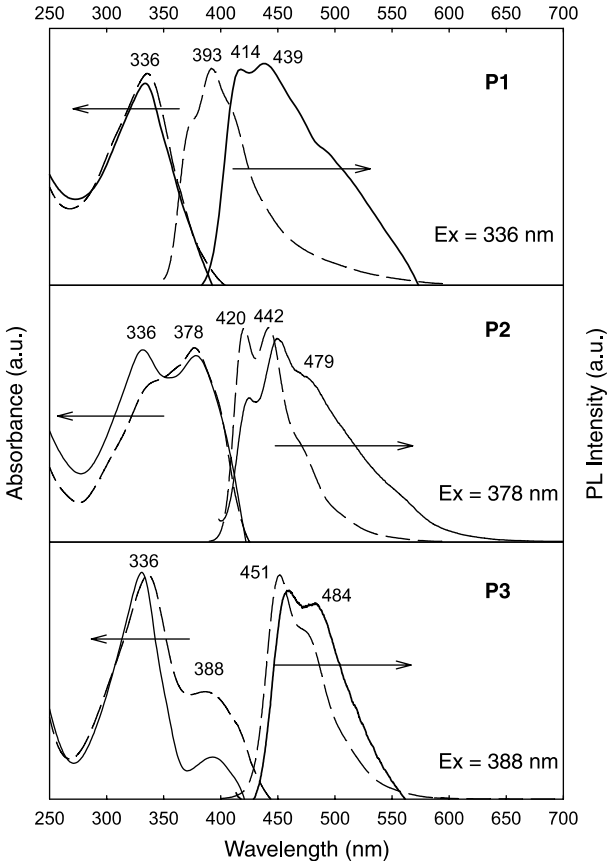

Fig. 2. Photoluminescence and UV–vis absorption spectra of polymers **P1**–**P3** in $CHCl_3$ solutions of 1×10^{-5} M (– – –) and in films coated on quartz plate (—).

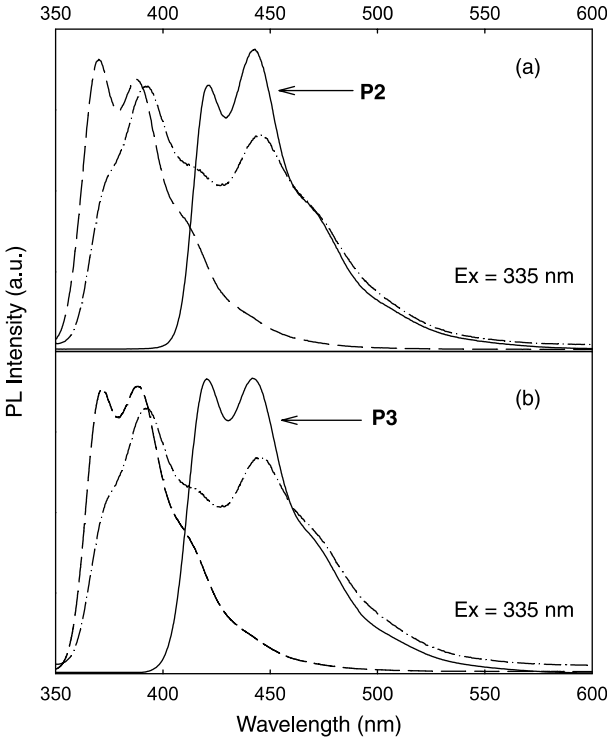

Fig. 3. Photoluminescence spectra of **P2**–**P3** (—: 1×10^{-6} M repeating unit) and mixture of model compounds. (a) **M1**+**M3**, (b) **M1**+**M4**; (– – –): 5×10^{-6} M, (– · –): 5×10^{-5} M in $CHCl_3$.

2,7-bis(3-(trifluoromethyl) phenyl)-9,9-dihexylfluorene segments to hole-transporting fluorophores during photo-excitation. The phenomena of energy transfer can be illustrated with absorption and photoluminescence of mixture composed of model compounds. As shown in Fig. 1, the emission spectra of **M1** cover greatly with the absorptions of **M3** and **M4**, respectively, suggesting that excitation energy may transfer from **M1** (energy donor) to **M3** and **M4** (energy acceptor) while the distance between donors and acceptors is short enough. In Fig. 3, under excitation with 335 nm (the absorption maxima of **M1**) the mixtures of **M1** and **M3** in $CHCl_3$ (5×10^{-5} M) exhibit not only emission around 390 nm (emission peaks of **M1**) but also a new peak around 440 nm attributed to **M3** [Fig. 3(a)]. Furthermore, the relative intensity of **M3** (at ca. 440 nm), as compared to that of **M1** (at ca. 388 nm), diminished significantly with reducing mixture concentration corresponding to raise intermolecular distances (from 5×10^{-5} to 5×10^{-6} M). Similar phenomena can be observed in mixture solution of **M1** (energy donor) and **M4** (energy acceptor) [Fig. 3(b)]. However, **P2** and **P3** show only emission of energy acceptors (2,7-distyrylfluorene and 1,4-distyrylbenzene segments) even under low concentration (10^{-6} M) when excited with 335 nm light (absorption maximum of **M1**). This is attributable to efficient intrachain energy transfer, because the energy donor and the energy acceptor are connected closely (only via ether spacers) and relative phenomena have been discussed in our previous works [19,22,35].

Comparing with their PL spectra in the solution, **P1**–**P3** in film states reveal red shift of ca. 46, 7, and 8 nm, respectively. The large PL shift in **P1** film is probably due to formation of interchain interaction. In order to discuss this phenomenon, the absorption and PL spectra of **P1** in mixture solution of methanol (poor solvent) and $CHCl_3$ (good solvent) has been measured. In Fig. 4(a), the absorption spectra of **P1** show only slight shift upon changing solvent composition. However, a new peak arises gradually around 446 nm in PL spectra [Fig. 4(b)] with increasing the methanol ratio. This phenomenon can be explained by stack or shrinkage of polymeric chains in poor solvent, which enhance local concentration of fluorophores and the formation of new emissive species. However, formation of aggregation can be excluded, since no obvious absorption shift can be observed. Therefore, the interchain interaction in **P1** can be proposed as formation of excimers [45,46].

Fig. 5 shows the PL spectra of **P1**–**P4** in film state after annealing at 100, 180 or 190 °C to examine their thermal

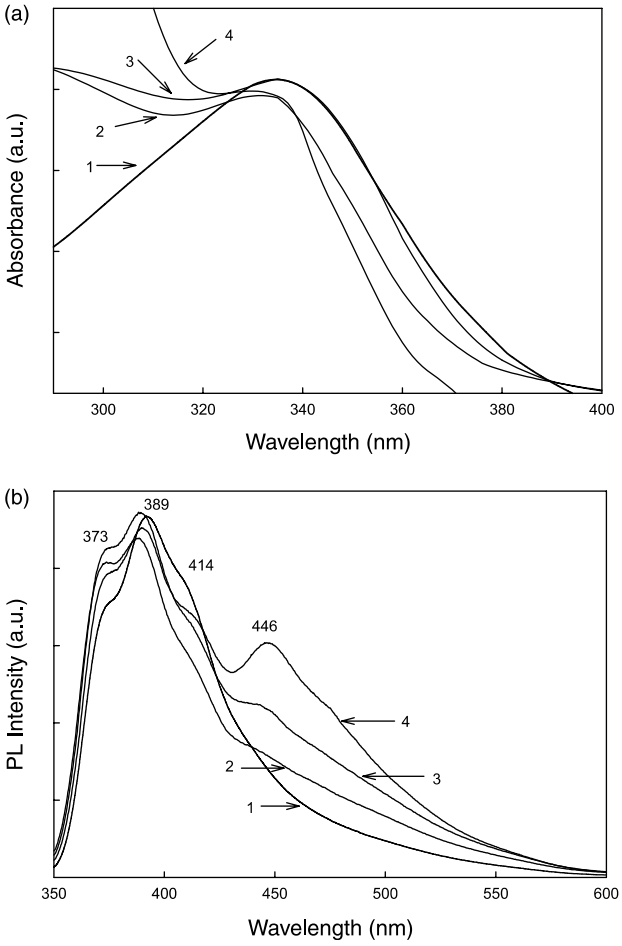

Fig. 4. (a) Absorption and (b) photoluminescence spectra of **P1** in mixture of MeOH and $CHCl_3$ at a concentration of 10^{-5} M. MeOH/$CHCl_3$ (v/v) = 0 (1), 0.2 (2), 0.5 (3) and 1 (4).

stability. Comparing to **P2**, the additional band around 550 nm in the PL emission of **P4** has been ascribed to excimer formation during annealing [35]. Therefore, it is suggested that the electron-transporting 2,7-distyryl-9,9-dihexylfluorene groups in **P2** provide great steric hindrance than 3,3‴-bistrifluoromethylquaterphenyl in **P4** and could reduce interchain interaction efficiently. There is also no new peaks can be found in **P1** and **P3** during heating at 100–190 °C. It is suggested that the emissions of **P1**–**P3** are thermally stable. As shown in Table 2, the relative quantum yields (Φ_{PL}) of **P1** ($\Phi_{PL}=0.33$) is much lower than these of **P2** and **P3** ($\Phi_{PL}=0.93$, 0.89), which can be attributable to intrinsic lower emissive efficiency of 3,6-distyrylcarbazole chromophores than 1,4-distyrylbenzene (**P3**) and 2,7-distyrylfluorene (**P2**) groups [22,25].

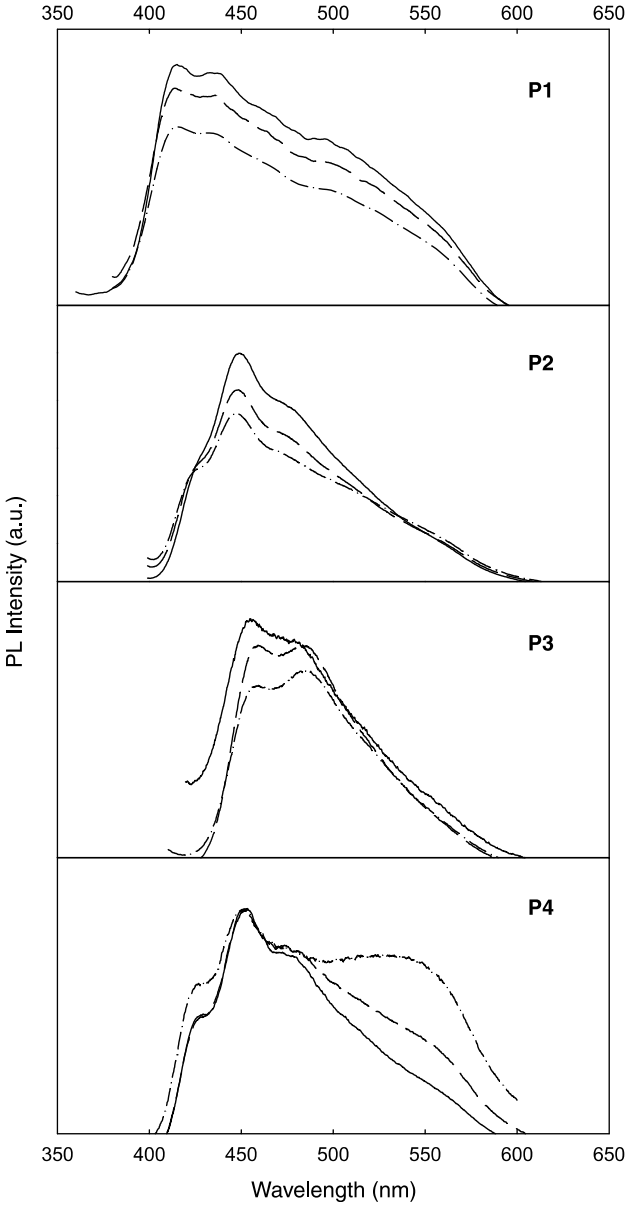

Fig. 5. Photoluminescent spectra of **P1**–**P4** in the film state after annealing at 100 °C for 1 h (—), 180 °C for 2 h (– – –) and 190 °C for 2 h (– · –) in vacuum.

3.3. Electrochemical property

In our previous studies about copoly(aryl ether)s with isolated alternate hole- and electron-transporting segments, we have verified that the reduction and oxidation start from electron- and hole-transporting segments, respectively [47]. Therefore, as shown in Table 3, contrary to fully conjugated polymers, the electrochemically estimated band gaps (E_g^{el}) of **P1**–**P3** are in the range of 2.09–2.32 eV, which are much smaller than those calculated from onset absorptions (E_g^{opt}) (2.76–3.15 eV).

The cyclic voltammorgams (CVs) of **P1**–**P3** are shown in Fig. 6. The reduction of **P1**–**P3**, starts similarly at −1.72 to −1.76 V, since they possess the same electron-transporting segments [bis(3-(trifluoromethyl)phenyl)-9,9-dihexylfluorene]. The onset oxidation potentials of **P1**–**P3** are at 0.45, 0.58, and 0.37 V, respectively. The highest occupied molecular orbital (HOMO)/lowest unoccupied molecular orbital (LUMO) levels and band gaps (E_g^{el}) of **P1**–**P3** can be calculated from their electrochemical data (Table 3). The HOMO and LUMO energy levels of **P1**–**P3** are −5.15, −5.28, −5.17 and −3.04, −3.06, −3.08 eV, respectively.

Furthermore, optical band gaps (E_g^{opt}) of **M1**–**M4**, calculated from their onset absorption, are 3.35, 2.90, 2.95 and 2.79 eV, respectively [25,35]. Therefore, the unabridged energy band diagrams of the copoly(aryl ether)s are proposed as Fig. 7. The LUMO levels of hole-transporting segments (top horizontal line of the broken rectangle) can be estimated from the HOMO levels of the copolymers by adding E_g^{opt}s of corresponding model compounds. For example, the LUMO level of hole-transporting segments in **P1** is estimated to be −2.25 eV by adding E_g^{opt} of corresponding **M2** (2.90 eV) with its HOMO level (−5.15 eV). The HOMO levels of electron-transporting segments (bottom horizontal line of the solid rectangle) can be estimated similarly. The electrochemically-determined band diagrams of **P1**–**P3** are the overlapped portions of corresponding model compounds. Therefore, hole and electron affinities of the isolated copoly(aryl ether)s can be promoted simultaneously. As shown in Fig. 7, the LUMO energy level of **P2** (−3.06 eV) is higher than **P4**, (−3.30 eV), indicating that the electron affinity of 2,7-bis(3-(trifluoromethyl)phenyl)-9,9-dihexylfluorene groups is less than 3,3‴-bistrifluoromethylquaterphenyl groups.

Double-layer EL devices (ITO/PEDOT/**P1**–**P3**/Al) were also fabricated and their electroluminescence spectra compared. As shown in Fig. 8, comparing to the PL spectra in film states, the EL of **P1** reveals obvious red-shift and shows a broader peak between 400 and 600 nm, which can be ascribed to the formation of interchain interactions during the application of voltage. Furthermore, the EL of **P2** reveals boarder peak and a shoulder around 560 nm similar to **P4**, which may also be attributable to the formation of

Table 3
Electrochemical data of **P1–P3**

No.	$E_{onset\ (red)}$ (V) vs. FOC	$E_{onset\ (ox)}$ (V) vs. FOC	E_{LUMO} (eV)[a]	E_{HOMO} (eV)[b]	E_g^{el} (eV)[c]	E_g^{opt} (eV)[d]
P1	−1.76	0.45	−3.04	−5.15	2.21	3.15
P2	−1.74	0.58	−3.06	−5.28	2.32	2.92
P3	−1.72	0.37	−3.08	−5.17	2.09	2.76

[a] $E_{LUMO} = -e(E_{onset\ (ox),\ FOC} + 4.8\ V)$.
[b] $E_{HOMO} = -e(E_{onset\ (red),\ FOC} + 4.8\ V)$.
[c] Band gaps obtained from electrochemical data.
[d] Band gaps obtained from UV/vis absorption spectrum.

excimers like that in **P4** during annealing. The optoelectronic characteristics of the EL devices with **P1–P3** as emitting layer are in progress and will be published later.

Although the hole and electron affinities of the isolated copoly(aryl ether)s were promoted simultaneously, the luminance of their EL devices was very low. This is probably due to the trapping of injected electrons and holes in electron- and hole-transporting segment, respectively. Furthermore, the ether spacers in the polymeric main chains function as barrier and decrease recombination of the carriers [22,25]. Therefore, the potential applications of **P1–P3** in EL devices should be as electron- or hole-transporting layers and the investigation is now in progress.

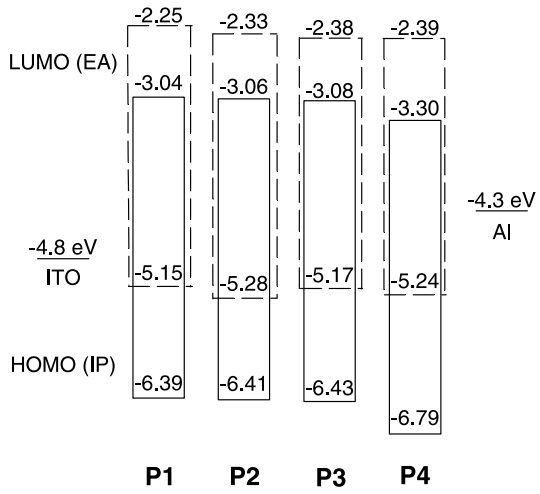

Fig. 7. The energy band diagram of **P1–P4** (hole transporting segments: —, electron transporting segments: – – –).

4. Conclusion

Three novel copoly(aryl ether)s **P1–P3** consisting of isolated electron-transporting and hole-transporting segments have been successfully synthesized and characterized. Comparing to model compounds, the PL spectra of **P1–P3** show maximum peaks at 393, 442, and 451 nm that can be ascribed to their alternate fluorophores (**P1**) or dominated by fluorophores with longer emissive wavelength via efficient energy transfer (**P2** and **P3**). Comparing to **P4**, **P2** possess less interchain interaction during annealing. From the cyclic voltammetric data, the HOMO levels of **P1–P3** are −5.15, −5.28, and −5.17 eV and the LUMO levels are −3.04, −3.06, and −3.08 eV, respectively. The LUMO and HOMO levels are controlled by 2,7-bis(3-(trifluoromethyl)phenyl)-9,9-dihexylfluorene segments and hole-transporting segments, respectively. Moreover, formation of interchain interaction in **P1** and **P2** has

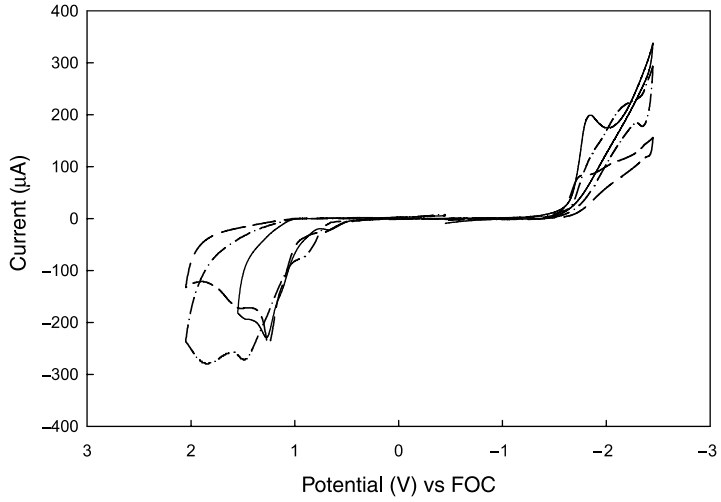

Fig. 6. Cyclic voltammograms of **P1** (—), **P2** (– · –), and **P3** (– – –) films coated on ITO glass at a scanning rate of 100 mV/s.

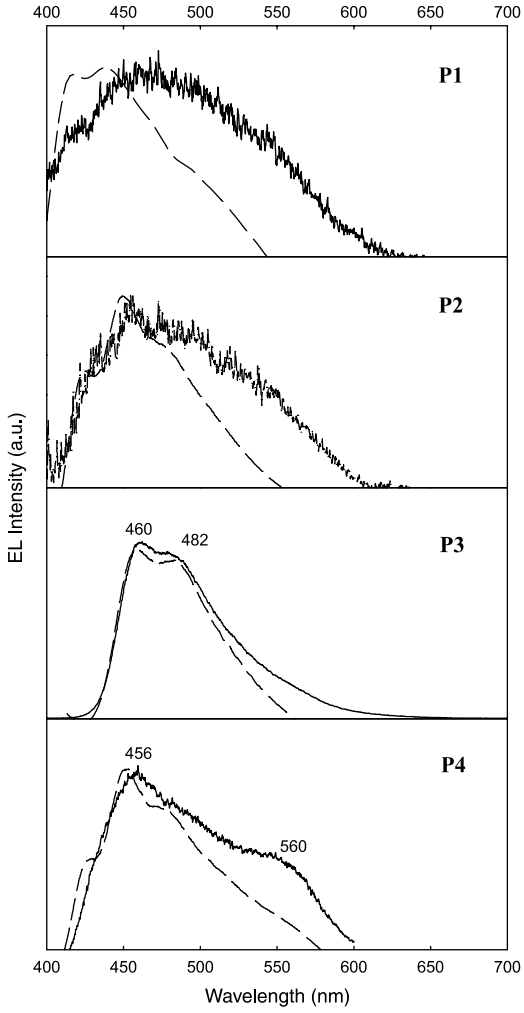

Fig. 8. Photoluminescent spectra (– – –) and electroluminscent spectra (—) of **P1**–**P4**.

been deduced from EL spectral investigation. The potential applications of **P1**–**P3** in EL devices will be as electron- or hole-transporting layers.

References

[1] Burroughes JH, Bradley DDC, Brown AR, Marks RN, Mackay K, Friend RH, et al. Nature 1990;347:539.
[2] Gustafsson G, Cao Y, Treacy GM, Klavetter F, Colaneri N, Heeger AJ. Nature 1992;357:477.
[3] Akcelrud L. Prog Polym Sci 2003;28:875.
[4] Liao L, Pang Y, Ding L, Karasz FE. Macromolecules 2002;35:3819.
[5] Shu CF, Dodda R, Wu FI, Liu MS, Jen AKJ. Macromolecules 2003; 36:6698.
[6] Mikroyannidis JA, Spiliopoulos IK, Kasimis TS, Kulkarni AP, Jenekhe SA. Macromolecules 2003;36:9295.
[7] Kraft A, Grimsdale AC, Holmes AB. Angew Chem Int Ed Engl 1998; 37:402.
[8] Lu HF, Chan HSO, Ng SC. Macromolecules 2003;36:9295.
[9] Mikroyannidis JA, Barberis VP, Ding L, Karasz FE. J Polym Sci, Part A: Polym Chem 2004;42:3212.
[10] Menon A, Dong H, Niazimbetova ZI, Rothberg LJ, Galvin ME. Chem Mater 2002;14:3668.
[11] Burn PL, Holmes AB, Kraft A, Bradley DDC, Brown AR, Friend RH, et al. Nature 1992;356:47.
[12] Hwang SW, Chen Y. Polymer 2000;41:6581.
[13] Hwang SW, Chen Y. Macromolecules 2002;35:5438.
[14] Zheng S, Shi J, Mateu R. Chem Mater 2000;12:1814.
[15] Machado AM, Neto JDDM, Cossiello RF, Atvars TDZ, Ding L, Karasz FE, et al. Polymer 2005;46:2452.
[16] Marko S, Rebecca HJ, Ananth D. J Am Chem Soc 1996;118:1213.
[17] Hidekaru D, Motoi K, Kenji O, Yasuhiko S. Chem Mater 2003;15: 1080.
[18] Cho NS, Hwang DH, Lee JI, Jung BJ, Shim HK. Macromolecules 2002;35:1224.
[19] Chen SH, Chen Y. J Polym Sci, Part A: Polym Chem 2004;42:5900.
[20] Chen SH, Hwang SW, Chen Y. J Polym Sci, Part A: Polym Chem 2004;42:883.
[21] Hwang SW, Chen Y, Chen SH. J Polym Sci, Part B: Polym Phys 2003; 42:333.
[22] Chen SH, Chen Y. Macromolecules 2005;38:53.
[23] Cho HJ, Jung BJ, Cho NS, Lee J, Shim HK. Macromolecules 2003;36: 6704.
[24] Chen ZK, Lee NHS, Huang W, Xu YS, Cao Y. Macromolecules 2003; 36:1009.
[25] Chen Y, Hwang SW, Yu YH. Polymer 2003;44:3827.
[26] Wu TY, Sheu RB, Chen Y. Macromolecules 2004;37:725.
[27] Liang F, Pu YJ, Kurata T, Kido J, Nishide H. Polymer 2005;46:3767.
[28] Ferreira M, Constantino CJL, Olivati CA, Balogh DT, Aroca RF, Faria RM, et al. Polymer 2005;46:5140.
[29] Tang R, Tan Z, Cheng C, Li Y, Xi F. Polymer 2005;46:5341.
[30] Kim YH, Ahn JH, Shin DC, Kwon SK. Polymer 2004;45:2525.
[31] Kim YH, Shin DC, Kwon SK. Polymer 2005;46:4647.
[32] Ho CC, Yeh KM, Chen Y. Polymer 2004;45:8739.
[33] Knupfer M, Fink J, Zojer E, Leising G, Scherf U, Mullen K, et al. Macromolecules 1999;32:361.
[34] Jin SH, Kang SY, Kim MY, Chan YU, Kim JY, Lee K, et al. Macromolecules 2003;36:3841.
[35] Hwang SW, Chen SH, Chen Y. J Polym Sci, Part A: Polym Chem 2002;40:2215.
[36] Kreyenschimdt M, Klaerner G, Fuhrer T, Ashenhurst J, Karg S, Chen W, et al. Macromolecules 1998;31:1099.
[37] Cirpan A, Ding L, Karasz FE. Polymer 2005;46:811.
[38] Assaka AM, Rodrigues PC, Oliveira ARM, Ding L, Hu B, Karasz FE, et al. Polymer 2004;45:7071.
[39] Sanda F, Nakai T, Kobayashi N, Masuda T. Macromolecules 2004;37: 2703.
[40] Lu J, Tao Y, D'iorio M, Li Y, Ding J, Day M. Macromolecules 2004; 37:2442.
[41] Cloutet E, Olivero C, Adès D, Castex MC, Siove A. Polymer 2002;43: 3489.
[42] Liu Y, Liu MS, Jen AKY. Acta Polym 1999;50:105.
[43] Kim HK, Ryu MK, Kim KD, Lee SM, Cho SW, Park JW. Macromolecules 1998;31:1114.
[44] Ahn T, Shim HK. Macromol Chem Phys 2001;202:3180.
[45] Zhang ZB, Fujiki M, Tang HZ, Motonaga M, Torimitsu K. Macromolecules 2002;35:1988.
[46] Takihana Y, Shiotsuki M, Sanda F, Masuda T. Macromolecules 2004; 37:7578.
[47] Hwang SW, Chen Y. Macromolecules 2001;34:2981.